

Geoff Bradway

Collaborators:  
Ben Ferguson  
Leah Moelling

## Introduction

*Falcarius utahensis* was a therizinosaur dinosaur that was discovered in the Yellow Cat formation, in Utah. Therizinosaurs were part of a much broader class of dinosaurs, theropods. *Falcarius* and other therizinosaur were primarily herbivorous, which challenged the notion that theropods were primarily hypercarnivorous ( Zanno, 2009).

*Falcarius* was excavated in the Crystal Geyser Quarry in Grand County Utah, which would date it to having lived about 126 million years ago in the early Cretaceous period (Kirkland, 2005). *Falcarius* helped shed new insight on the shift from carnivory to herbivory in Therizinoidea ( Zanno, 2009). *Falcarius* is the earliest known therizinosaur, so it represents a good transitional fossil between hyper carnivorous theropods and the only known branch of primarily herbivorous theropods (Zanno, 2010). As a result, the physiological structure, osteological structure , and lifestyle of *Falcarius* are of great interest because it represents the drastic transition from a well adapted carnivorous form to the herbivorous form. This can be seen in the mixture of traits that *Falcarius* possesses, such as regression in cursorial adaptations on its hind limbs (Zanno, 2009).

Typically therizinosaurioids had long necks, laterally expanded pelves, small leaf shaped teeth, large claws on their hands, and hind feet with four toes. Their forelimbs supported a range of motion that is not seen in other theropods (Burch, 2006) .

*Falcarius* was a slender smaller theropod, about four meters long and one meter high at the hip (Kirkland, 2005) . It is believed to be a transition to a more herbivorous omnivore because of its teeth and an osteological hind limb structure designed to support large weight (Zanno, 2009). *Falcarius* has an increased number of digits on its hindlimbs believed to help support weight, and a shortening of the tibia relative to the femur, both of which are a reversal of cursorial adaptations. This dinosaur has small leaf shaped teeth likely with a keratin beak, which is seen in other herbivores. In addition, *Falcarius* had a displaced pubis with an expanded pelvis which suggests an increase in intestinal mass (Kirkland 2005). All of these suggest a slower moving dinosaur, which suggests more of a herbivore than a carnivorous predator.

With reconstruction techniques and computational simulations, we can hope to gauge this change in overall form from a well adapted carnivore to a herbivore. We used photogrammetry to first establish a working 3D model of *Falcarius* to use for simulations. Photogrammetry is using a series of photographs to generate a 3D model. Intuitively this process is similar to how our eyes utilize stereoscopic vision to generate a 3D view.

With this 3D model, we can then analyze body features that allude to lifestyle. Since presently there are many allometric mass curves to describe features in extant animals, we started by using volumetric reconstructions from the skeleton to gauge

a range of body mass. We used modeling and mathematical software to generate a range of viable volumes, and extant animal physiological densities to deduce a range of masses.

To test the viability of *Falcarius* as a predator we analyzed a wide range of aspects. We reconstructed a hindlimb to examine the structure for cursorial adaptations. If *Falcarius* is this transition between these predators and the slow moving therizinosaurus, we should be able to see a decrease in cursorial aptitude. Furthermore, to analyze what the likely speed of *Falcarius* would have been, we reconstructed M. caudofemoralis in *Falcarius*. This muscle is an integral part of the movement in many extant reptiles, such as alligators, and size helps determine maximum movement. Such a reconstruction then can help us determine agility and athleticism in *Falcarius*, and while the presence of such features can not help us determine carnivorous versus herbivorous behavior, the lack of such features would imply herbivorous or scavenger behavior, since it would unlikely that this dinosaur could have efficiently caught prey .

Next we used computational models to simulate bite force in extant alligators to try and predict what the likely bite force in *Falcarius* would have been. Clearly a high bite force can be linked with predatory behavior, whereas a low bite force might allude to either herbivorous or possibly scavenger behavior. We used juvenile alligators due to the similarity in skull size.

Next we used extant animal data and our previous estimate to model the cardiac and respiratory system of *Falcarius*. This allows use to assess if the cardiac output would have been sufficient to support a high activity lifestyle. The cardiac output cannot imply much about predatory or herbatory behavior since there are extant animals of both classes with high and low cardiac output. However, the cardiac capabilities does shed light on the lifestyle this dinosaur would have lived given either behavior.

Finally we analyzed the inner ear structure of this dinosaur. This allows us to infer about the auditory capabilities of this dinosaur, which then imply information about its lifestyle. A well developed auditory system could be easily utilized in any life style, but it also suggests a high degree of sociability (Walsh 2008), which would have implications about the predatory or herbatory structure used.

## Photogrammetry

### Materials and Methods:

In order to fully calibrate the software system for classroom use, the technique was applied to variety of objects, ranging from drastically different sizes, and utilizing different cameras. As the technique is virtually the same for all of these, the process will be described in general. The process of producing a 3D model from a specimen can be given by the following:

1. Acquisition of the photographs of the specimen.
2. Production of a sparse point cloud.
3. Production of a dense point cloud.
4. Post processing.

#### 1. Acquisition of photographs

The three type of cameras that were used were the Pentex Optio S5i, Nikon D3000, and the Canon EOS Digital Rebel XT. The camera choice was based off of the availability and not off of any technical specifics.

The number of photographs to generate a viable model ranged greatly based upon camera choice and model complexity. In order to generate a good model, every point photographed has to be in at least three photographs from three different positions (Falkingham, 2012). For the best results, photographs every 15 degrees around the specimen is recommended (at least 24) (Falkingham, 2012). Also ideally, there should be a ~50% overlap in photos (Falkingham, 2012).

## **2. Production of a sparse point cloud / 3. Production of a dense point cloud**

The sparse point cloud was produced with a freeware software called Bundler. For installation specifics see the installation appendix (after references). The Bundler package that is available is all inclusive. The basic Bundler package generates a sparse point cloud, and the PMVS and CMVS (Patch-based Multi-view Stereo system and Clustering Views for Multi-view Stereo) are two methods to generate a point cloud from the sparse point cloud. PMVS is used for smaller photo sets while CMVS is used on larger photo sets and calls PMVS first. For this paper we used PMVS.

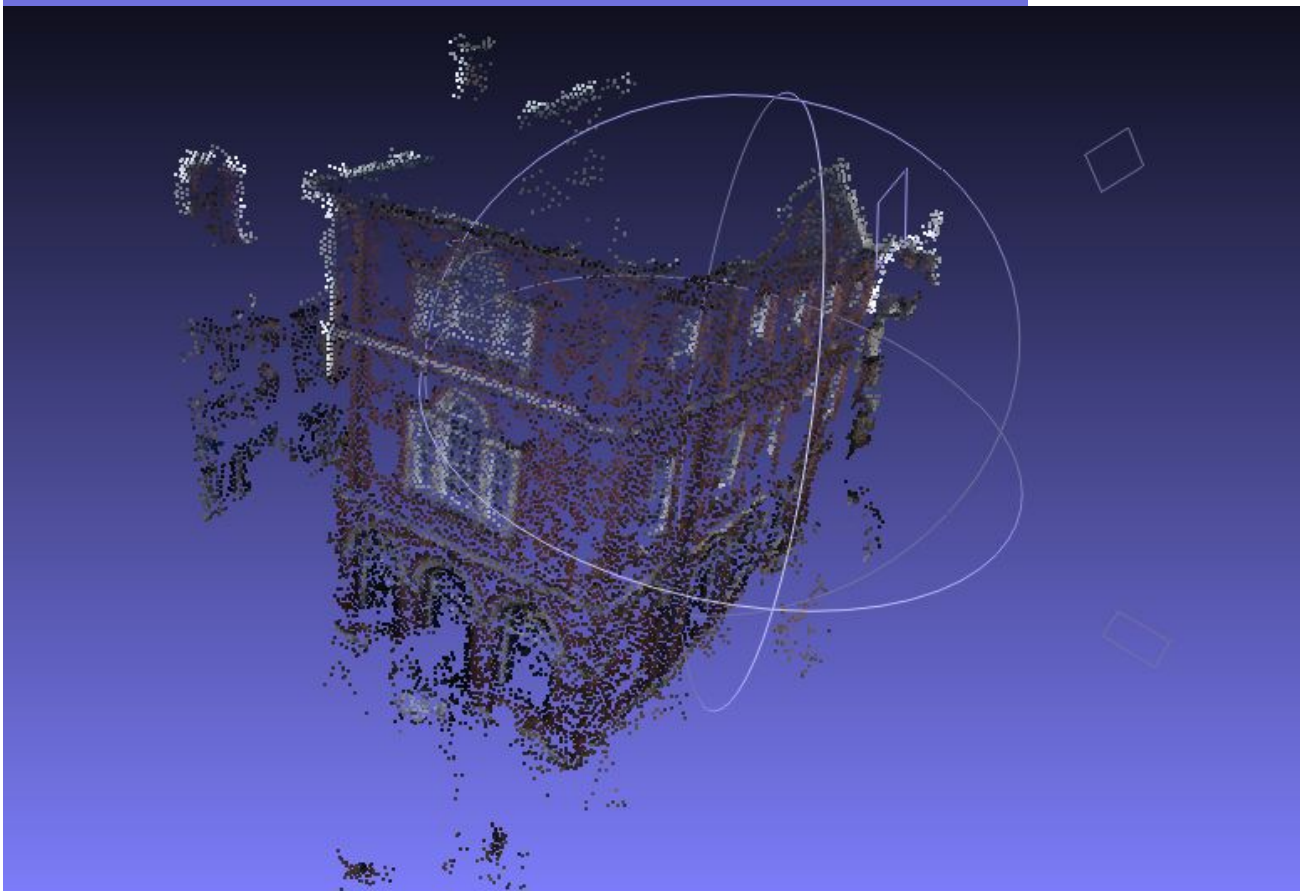
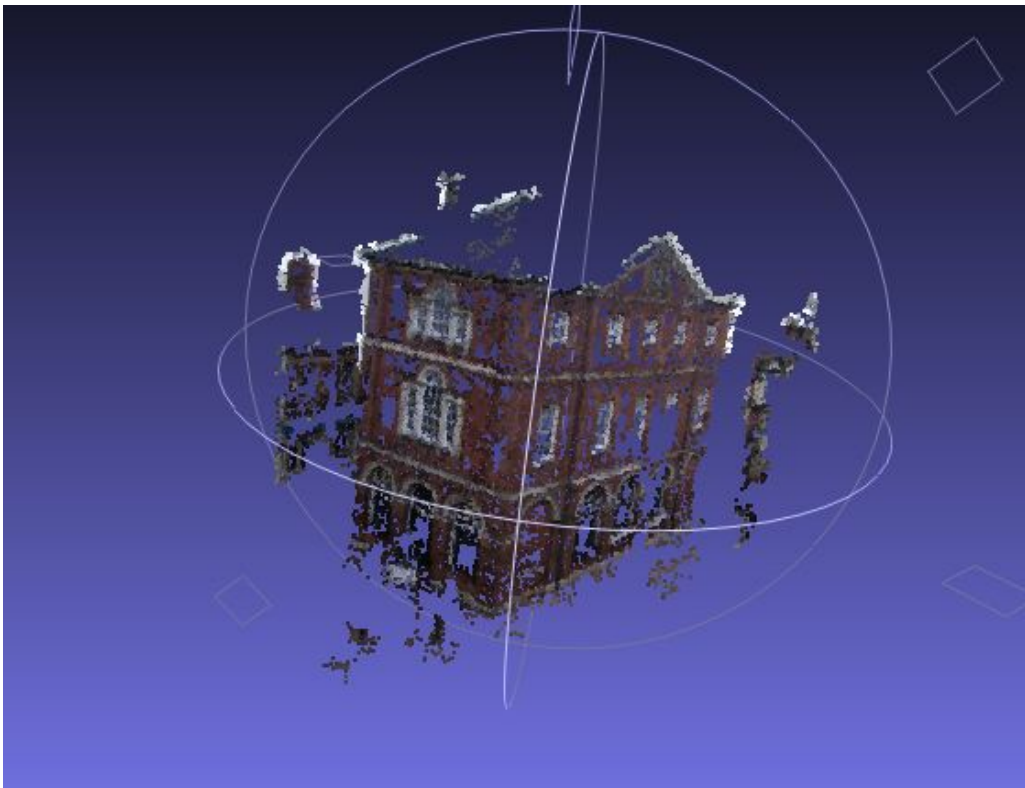
## **4. Post processing**

The file that is outputted by the PMVS script is a .PLY which is a CAD file that can be opened and read by many computer programs. For this test, we used the free software MeshLab. Since the 3D model was taken with photographs there are a couple of negative results. First off, the result is scaleless, so some sort of scale has to be known beforehand, or included while sampling the specimen. Also the software will reconstruct extraneous objects in the background, but these can be readily deleted. However, we have found that it useful to have objects in the background as it readily provides key points to help the software calibrate the photos. After this, the model can be treated as if it were a laser scanned model.

Results (figures included):

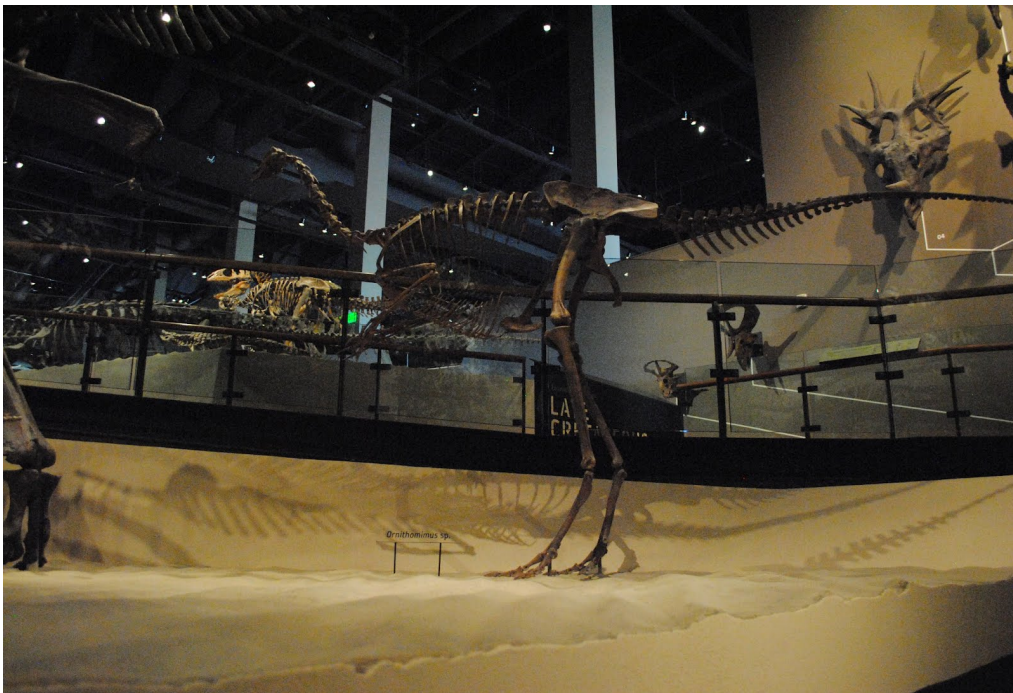
For the first set, we tried the sample photos included in the software. There were four photos and I got the following model. This was with the Pentex Optio S5i.

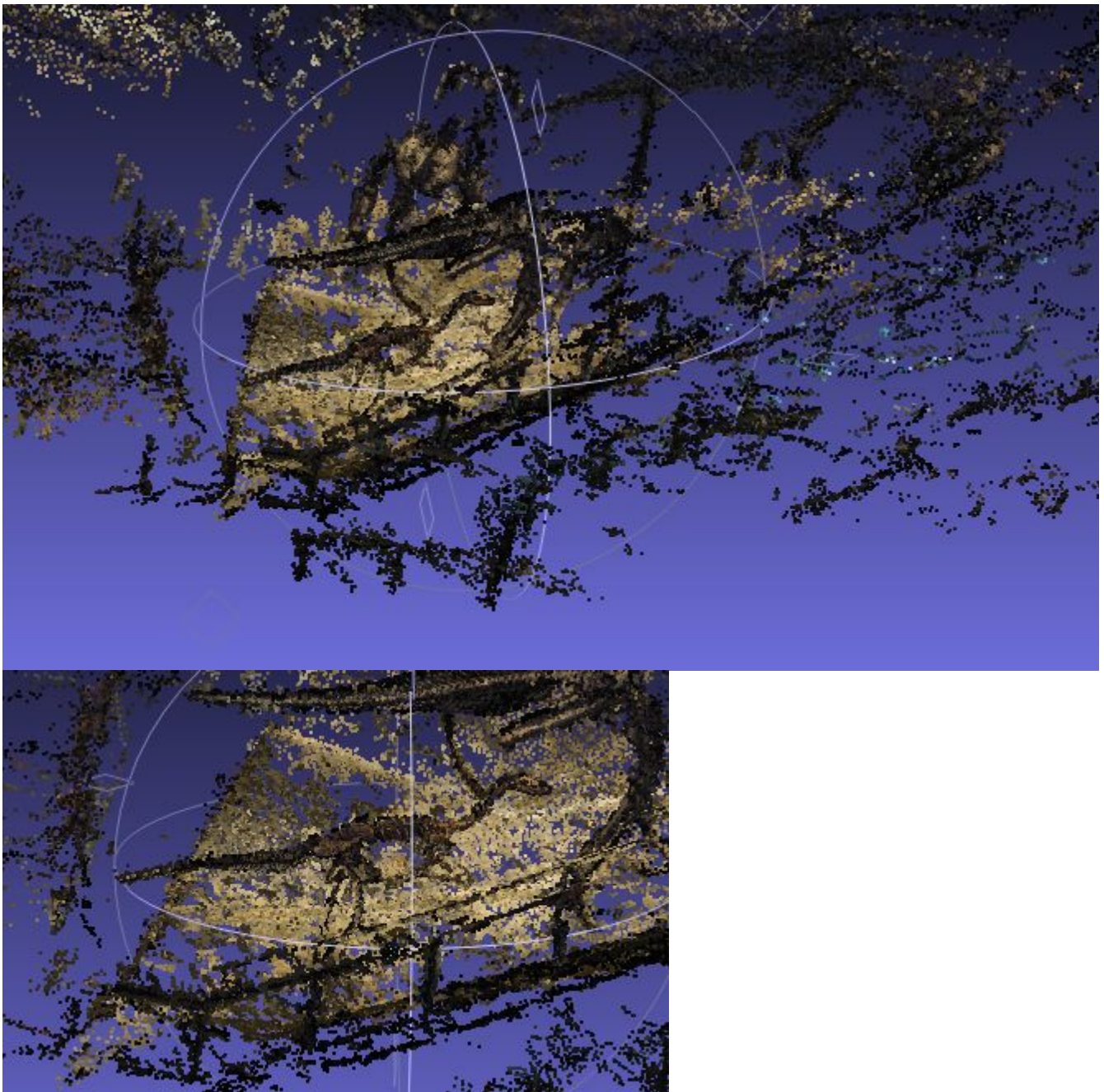


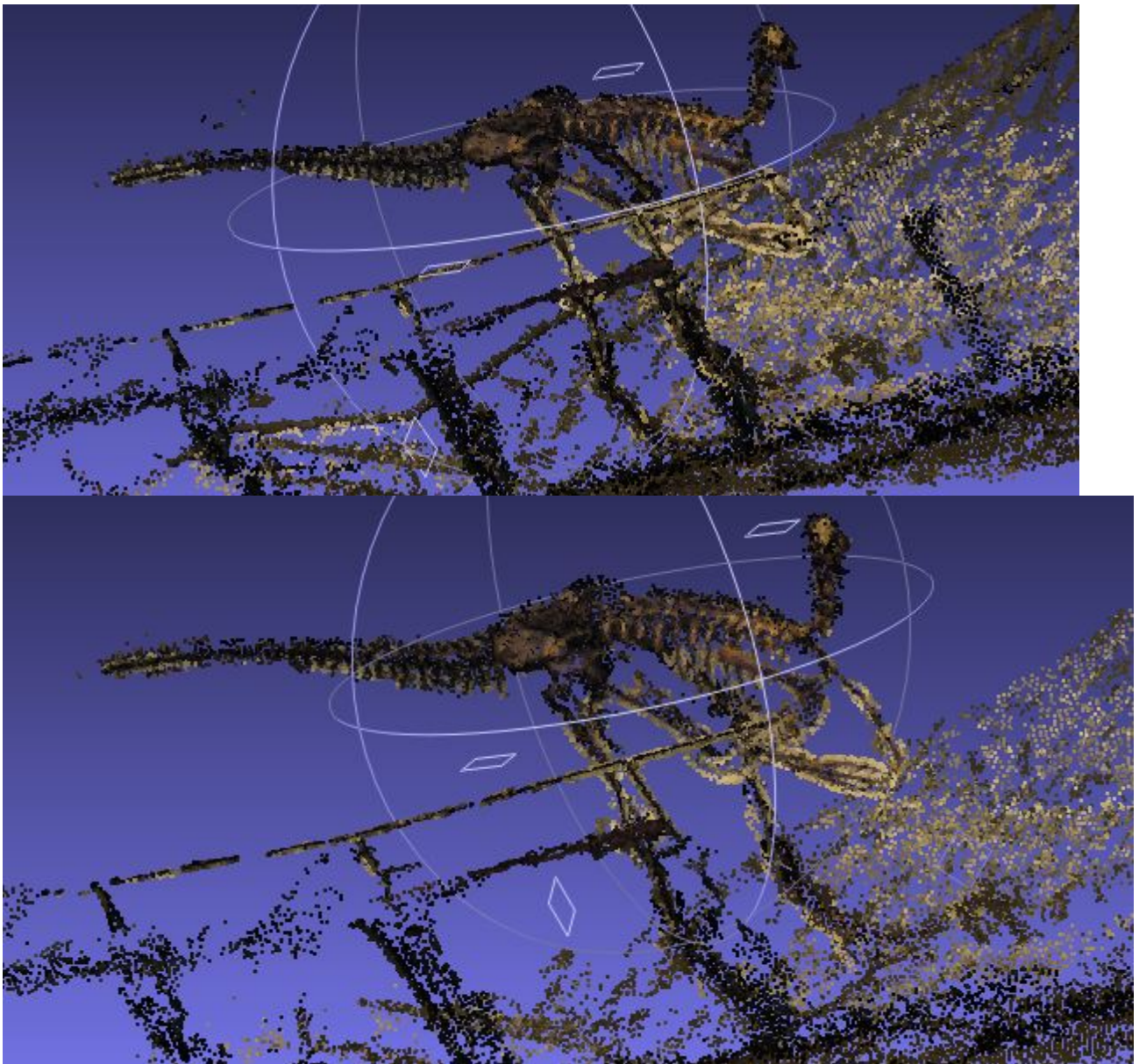




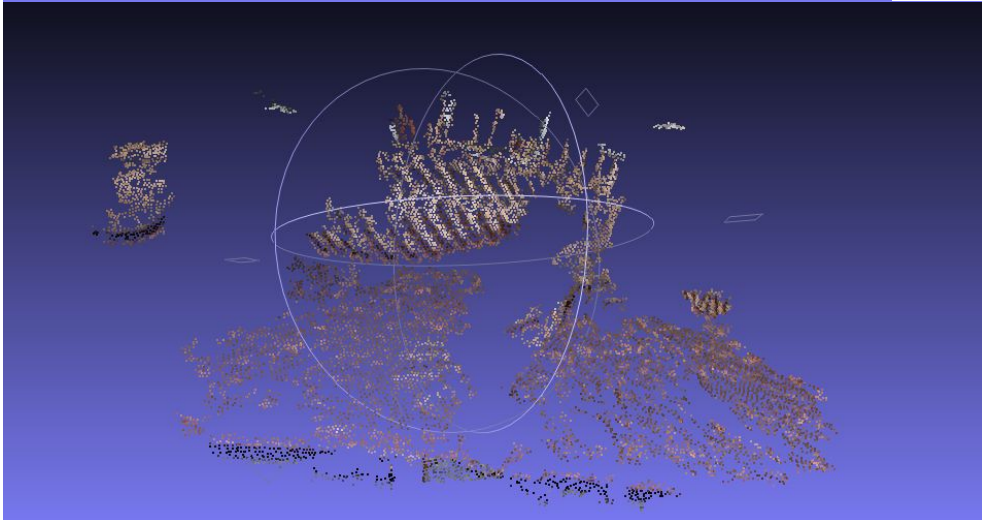
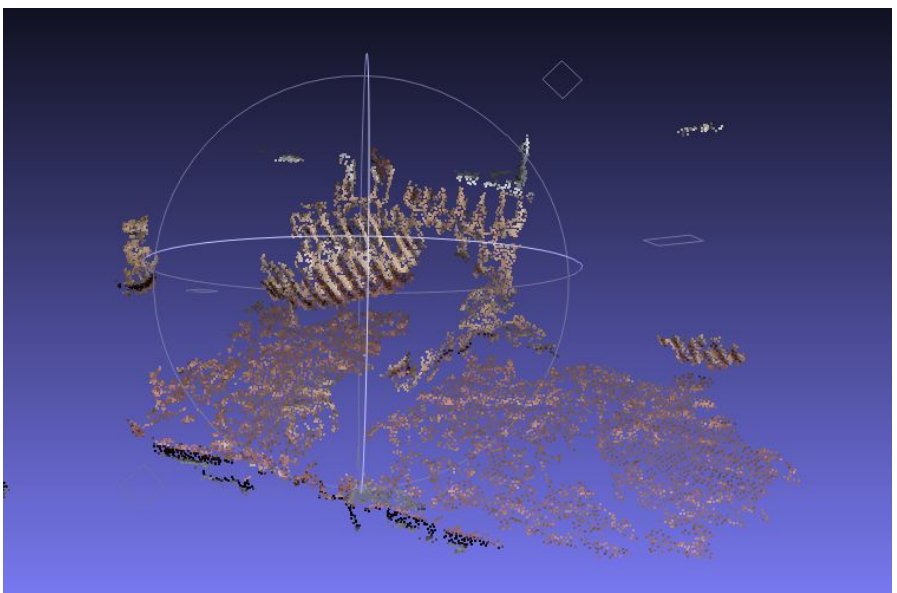
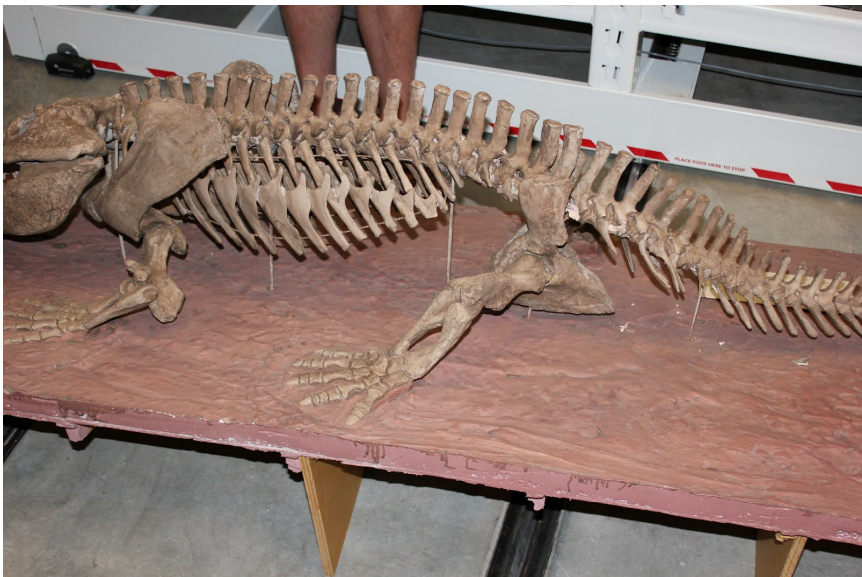
For my second set we used about 200 photos we had of an ornithopod taken in the museum. These were taken with a Nikon D3000.





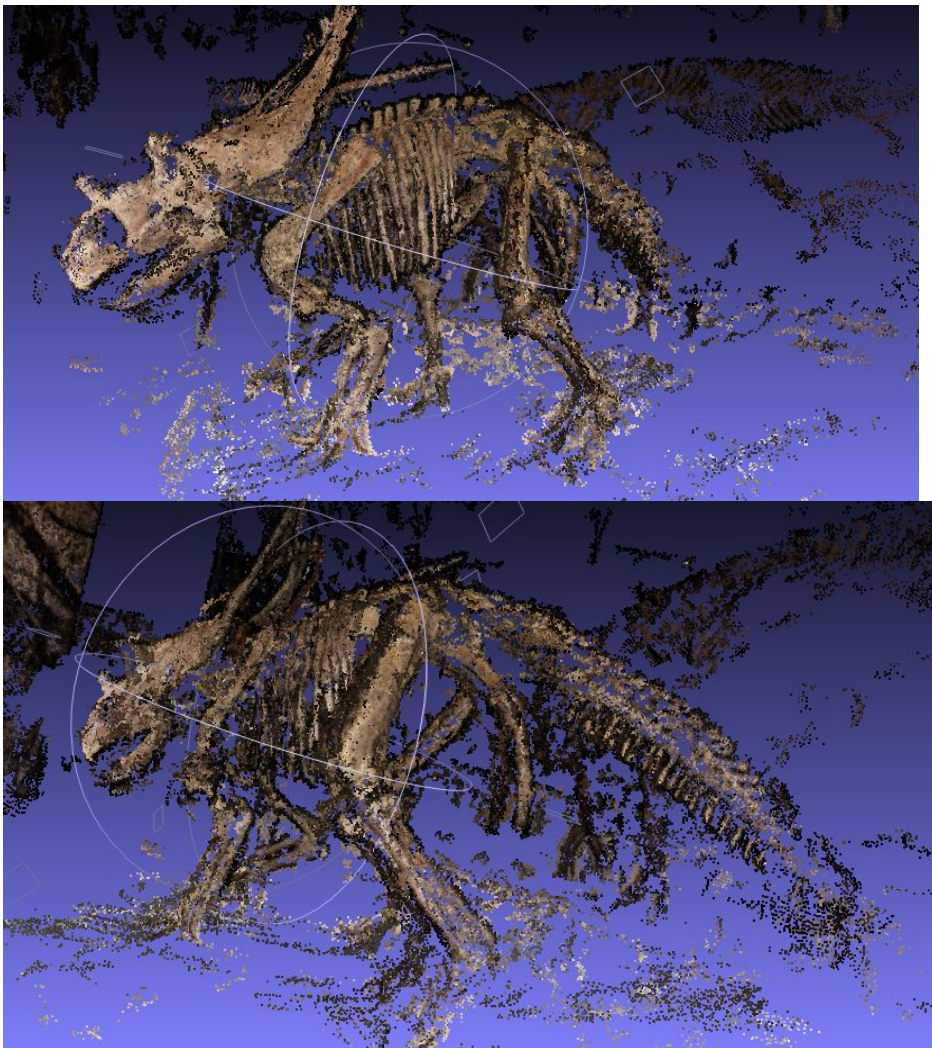


Next with a small photoset ( about 40 photos) of an amphibian, taken in the UMNH, we got the following results. This was taken with a Canon EOS Digital Rebel XT. Unfortunately we did not get optimal results. This is due to the limited exposure range, few misc background objects (helps determine positions and scale) and not enough overlap in photos.



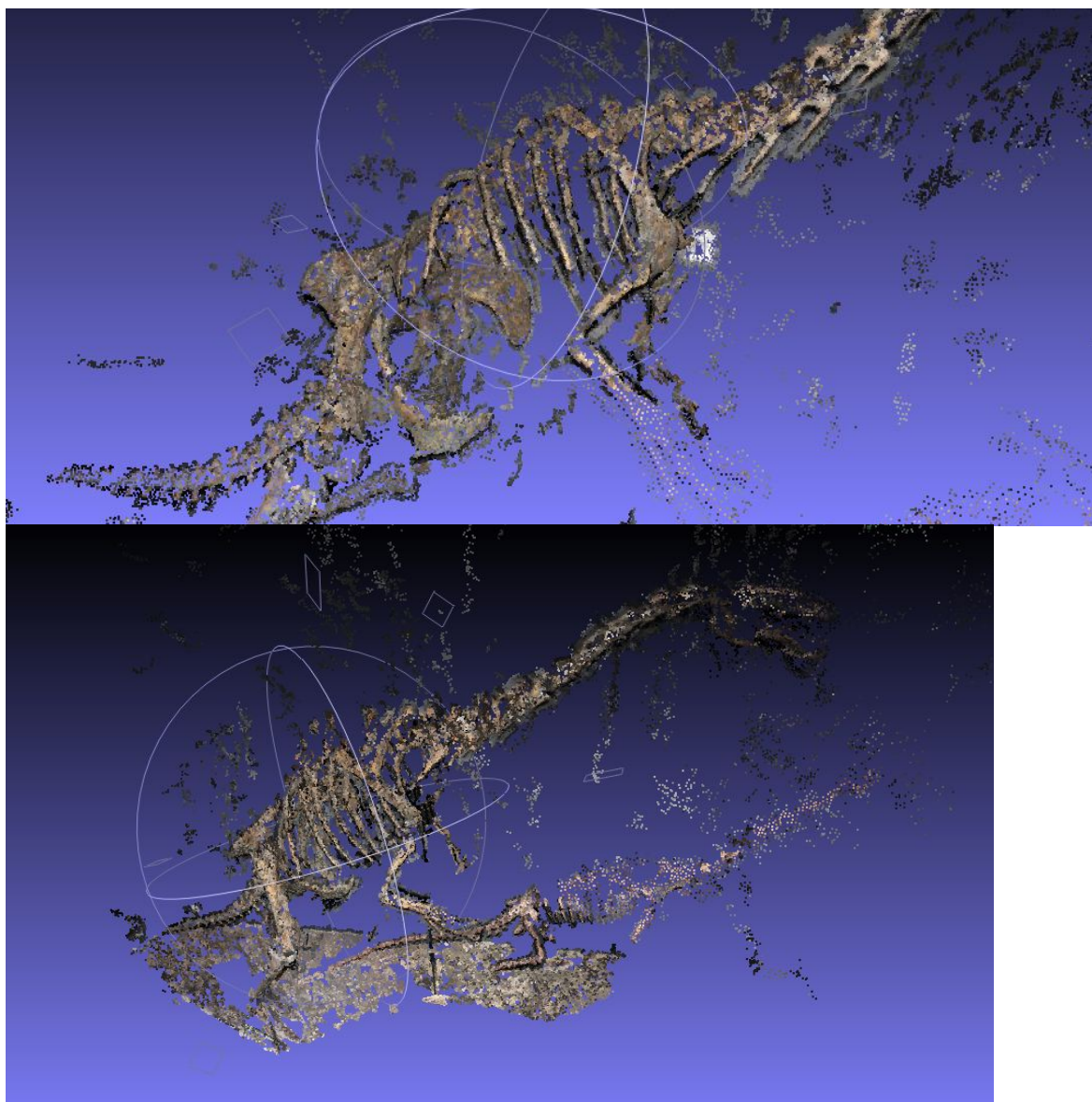
Next with a photoset ( about 100 photos) of an ceratopsian, taken in the UMNH, we got the following results. This was taken with a Canon EOS Digital Rebel XT.

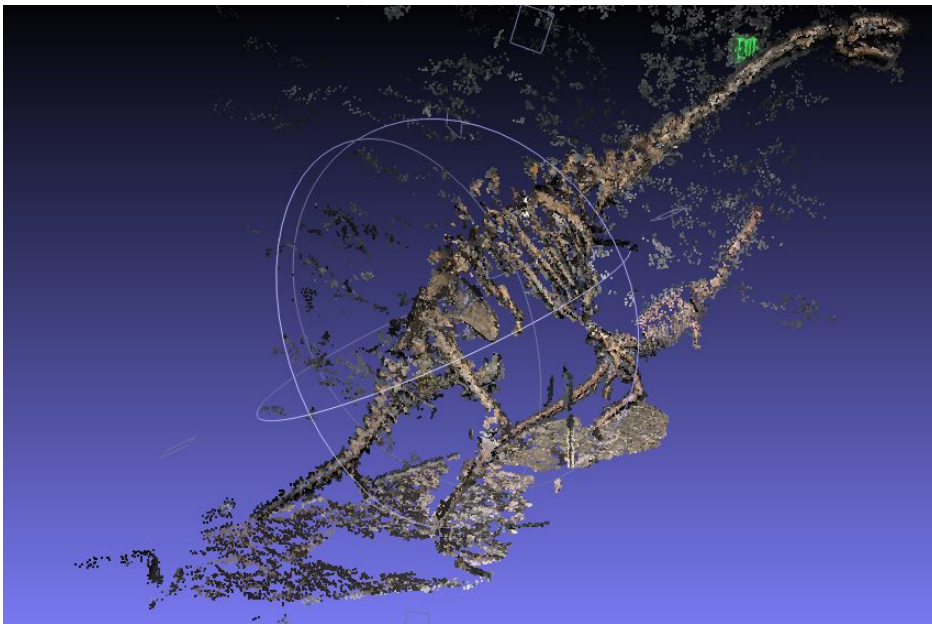




Finally with a photoset ( about 150 photos) we were able to generate *Falcarius*, taken in the UMNH, we got the following results. This was taken with a Canon EOS Digital Rebel XT.







## Volumetric Reconstruction

### Materials and methods:

For the skeletal models for the volumetric reconstruction we used models obtained by RIEGL LMS-Z420i 3D terrestrial Light Detection and Range (LiDAR) scanner (Hutchinson, 2011). For a more detailed insight on how the models were obtained, see (Bates, 2009) or (Hutchinson, 2011). The reason that we used a scanner and not photogrammetry was due to time constraints coupled with improper use of the photogrammetry software, and we had scanned models on similar dinosaurs.

For the model handling we used Maya 2012 (Bates, 2009). Then we used a MatLab script to determine the smallest convex volume around a given set of bones. A convex set is a set in which if X and Y are points in the set, then the line from X to Y is contained in the set. Then we would partition the skeleton into sets where a convex volume surrounding it seemed physiologically likely based off of extant animal proportions. We did this for the entire skeleton and used this to derive the minimum possible mass. We then adjusted the volume of these minimized portions to derive reasonable estimates for volume, and estimates that were believed to be overestimates. Finally we would estimate the average volume density in a section, ie a jaw is mostly bone, but some muscle, so an approximation of 80% bone and 20% muscle was used. The densities used for muscle were  $1006 \text{ kg/m}^3$  and for bone was  $1500 \text{ kg/m}^3$ . Finally we also adjusted each proportion to try to create a caudal and cranial centered animal.

We did this volumetric analysis on *Tyrannosaurus Rex* to compare our methodology with that of current literature, namely (Hutchinson, 2011). Then, we reran the method on *Plateosaurus* due to the resemblance of *Falcarius* in body form.

### Results:

For *Tyrannosaurus Rex* the predicted range was from ~6150- 12550 kg. Similar computational estimates that a typical Trex was around 6000-8000 kg, while "Sue", the largest found instance of *Tyrannosaurus Rex*, would have weighed

around 9500 kg (Hutchinson, 2011). As we can see, the lower end of our ranges are similar, while upper range is vastly different, however if we include Hutchinson's value for a maximal value, we get that ranges are similar.

For the normalization we got the following results as compared to Hutchinson's the following results. ( For the comparison we used the the Trex with similar mass from Hutchinson, as he tested it with multiple models). As we can see the results are somewhat close in the cranial and max model. However for the caudal and minimizing model have off with their COM X. Since we reused a lot of parts in the caudal model from the minimizing model it's probable that we made a mistake on a more cranial body part that is present in both. Note that the COM X,Y are relative to the hip joint and the normal X, and Y have been normalized with the femur length.

	Mass	COM X	COM Y	normal X	norm Y
Caudal	6830	-0.346	-0.381	-27.1	-29.9
Hutchinson Stan (most ventral)	7746	0.378	-0.63	29.5	-49.9
Cranial	9100	0.556	-0.351	43.6	-27.5
Hutchinson Carnegie (most ventral)	8888	0.447	-0.388	35.3	-30.7
Min	6158	-0.029	-0.410	-2.2	-32.1
Hutchinson Stan (min)	5934	0.524	-0.49	41.0	-38.7
Max	12564	0.236	-0.519	18.5	-40.7
Hutchinson Sue( most caudal)	13691	0.116	-0.35	13.6	-24.7

For *Plateosaurus* we conclude that the most reasonable mass estimate was about ~735 kg. Since *Plateosaurus* was roughly twice the size of *Falcarius* that means

that the volume would have been off by a factor of eight. This means that *Falcarius* would have weighed ~91.875 kg, and this is within 10% of the literature value of 100 kg (Paul, 2010). This means that our method provides data that is consistent with the previously done work, and so *Falcarius* weighed around 100 kg.

## Hindlimb Reconstruction

### Materials and Methods:

We used the skeletal reconstruction that Hartman did for the Utah Museum of Natural History, combined with the figure he designed which included a lateral view of *Falcarius* that had likely body proportions ( see figure HR.1). With this diagram we divided the limb into 23 sections perpendicular to the long axis of the limb(see figure HR.2). Next we estimated an aspect ratio [ anterior-posterior to medio-lateral diameter] to seven limb intermediate sections (see figure HR.3). To determine the intermediate aspect ratios we simply used a line connecting the two values, ie if section one had an aspect ratio of 2:1.5 and section 3 had 1.5:1 then we assumed section 2 had 1.75:1.25. Now assuming that thickness is constant in each section, we can determine the volume of bone and flesh. Assuming bone has a density of 1500 kg/m<sup>3</sup> and muscle has a density of 1006 kg/m<sup>3</sup> we can then approximate mass of each section. Finally we can estimate the center of mass for each section ( see fig HR.2) and use this to derive moment of inertia for the total limb.

### Results:

For the derived measurements we got the following results:

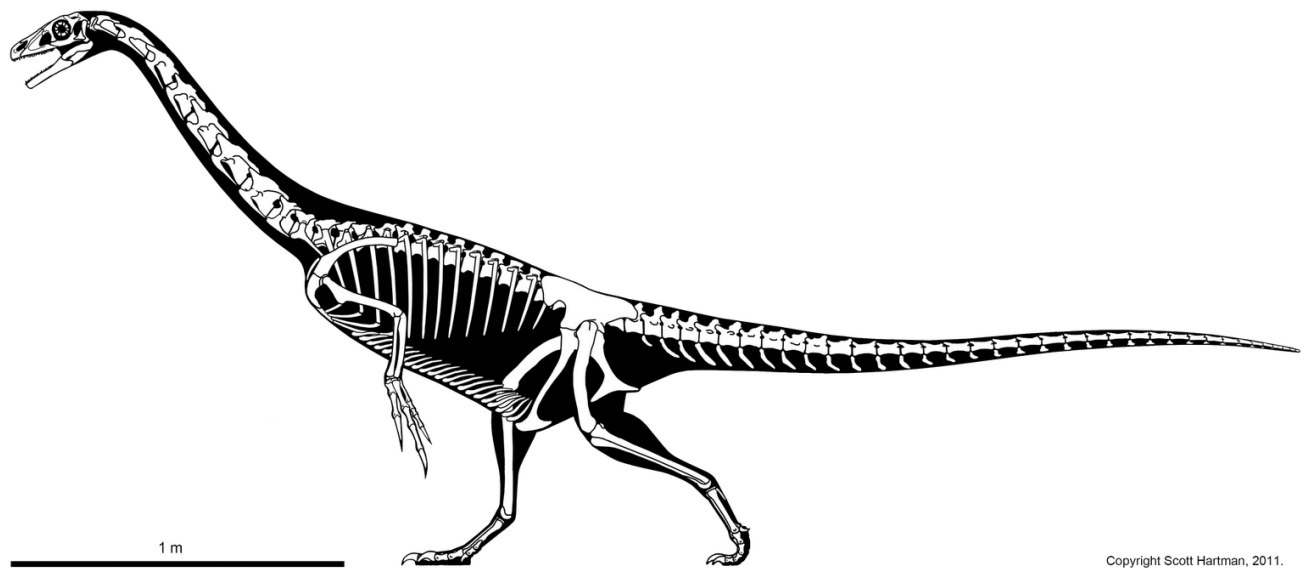
Section	Aspect Ratio(A/B)	Bone diameter (unscaled)	Leg Diameter (unscaled)	Distance (unscaled)	Scaling factor (scales to meters)	BD(scaled)	LD(scaled)	Distance(scaled)	A	B
1	1.53846153846154	1.3	4	0.6	0.04273504273504	0.0555555555555555	0.17094017094017	0.02564102564102	0.08547008547008	0.0555555555555555
2	2.1	1	4.5	1.5	0.04273504273504	0.19230769230769	0.06410256410256	0.09615384615384	0.04578754578754	
3	2.66	0.9	4.5	2.4	Thickness	0.03846153846153	0.19230769230769	0.10256410256410	0.09615384615384	0.03614806246385
4	3.22222222222222	0.8	4.3	3.4	1	0.03418803418803	0.18376068376068	0.14529914529914	0.09188034188034	0.0285145885941
5	2.75	0.8	4.1	4.4	0.03418803418803	0.17521367521367	0.18803418803418	0.08760683760683	0.03185703185703	
6	2.28	0.8	3.6	5.4	Scaled thickness	0.03418803418803	0.15384615384615	0.23076923076923	0.07692307692307	0.03373819163292
7	1.81818181818182	0.8	2.7	6.3	0.04273504273504	0.03418803418803	0.11538461538461	0.26923076923076	0.05769230769230	0.03173076923076
8	1.77	1.2	3	7.5	0.05128205128205	0.12820512820512	0.32051282051282	0.06410256410256	0.03621613791105	
9	1.73	0.9	3.2	8.2	0.03846153846153	0.13675213675213	0.35042735042735	0.06837606837606	0.03952373894570	
10	1.687	0.7	2.8	8.8	0.02991452991453	0.11965811965812	0.37606837606837	0.05982905982906	0.03546476575522	
11	1.64	0.6	2.1	9.6	0.02564102564102	0.08974358974359	0.41025641025641	0.04487179487179	0.02736085053158	
12	1.6	0.6	1.9	10.4	0.02564102564102	0.08119658119658	0.44444444444444	0.04059829059829	0.02537393162393	
13	1.35555555555556	0.5	1.2	11.3	0.02136752136752	0.05128205128205	0.48290598290598	0.02564102564102	0.01891551071878	
14	1.11111111111111	0.5	1.2	12	0.02136752136752	0.05128205128205	0.51282051282051	0.02564102564102	0.02307692307692	
15	1	0.6	1.4	12.9	0.02564102564102	0.05982905982906	0.55128205128205	0.02991452991453		
16	1	0.6	1.3	14	0.02564102564102	0.05555555555555	0.59829059829059	0.02777777777777	0.02777777777777	
17	1	0.6	2	15.8	0.02564102564102	0.08547008547008	0.67521367521367	0.04273504273504	0.04273504273504	
18	1	0.5	1.2	16.3	0.02136752136752	0.05128205128205	0.69658119658119	0.02564102564102	0.02564102564102	
19	1	0.5	1.2	17.3	0.02136752136752	0.05128205128205	0.73931623931623	0.02564102564102	0.02564102564102	
20	1	0.5	1.3	18.3	0.02136752136752	0.05555555555555	0.78205128205128	0.02777777777777	0.02777777777777	
21	1	0.3	0.7	19.3	0.01282051282051	0.02991452991453	0.82478632478632	0.01495726495726	0.01495726495726	
22	1	0.3	0.8	19.8	0.01282051282051	0.03418803418803	0.84615384615384	0.01709401709401	0.01709401709401	
23	1	0.1	0.6	19.5	0.00427350427350	0.02564102564102	0.83333333333333	0.01282051282051	0.01282051282051	

Then we can figure out the inertia with a cursorial sensitivity ( +- 5% mass on the foot):

Section	Bone cross section	Muscle cross section	Mass	Inertia
	pi*radius^2	pi*a*b-BCS	Scaled thickness*(MCS*1000+BCS*1500)	mass*distance^2
1	0.00242406840554	0.01491734403414	0.796707295156664	0.00052380492778
2	0.00143436000328	0.01383132860308	0.68657506750535	0.00282123219717
3	0.00116183160265	0.01091946894980	0.543920263824332	0.00572171217898
4	0.00091799040210	0.00823075338435	0.412697585803909	0.00871280807037
5	0.00091799040210	0.00876785151097	0.435788214666335	0.01540810109566
6	0.00091799040210	0.00815320422918	0.40936363494498	0.02180043026334
7	0.00091799040210	0.00575106643316	0.30609224080821	0.02218715946686
8	0.00208547840472	0.00729335594889	0.445954431268322	0.04581221557243
9	0.00116183160265	0.00849008464370	0.439477459639247	0.05396753668299
10	0.00070283640160	0.00666590540944	0.331630574543409	0.04690165770443
11	0.00051636960118	0.00385702903321	0.198919897828603	0.03348027208686
12	0.00051636960118	0.00323627475740	0.172232769560836	0.03402128781449
13	0.00035859000082	0.00152371357725	0.088493199143255	0.02063645371941
14	0.00035859000082	0.00185893056425	0.10290466448166	0.02706237067236
15	0.00051636960118	0.00281134560643	0.153964447942104	0.04679162791665
16	0.00051636960118	0.00242406840554	0.137314838365538	0.04915207158968
17	0.00051636960118	0.00573744001313	0.279761498076155	0.12754704576818
18	0.00035859000082	0.00208547840472	0.111784456255828	0.05424065341261
19	0.00035859000082	0.00208547840472	0.111784456255828	0.06110009846009
20	0.00035859000082	0.00242406840554	0.127200761419315	0.07779652091408
21	0.00012909240029	0.00070283640160	0.038491111985526	0.02618444426818
22	0.00012909240029	0.00091799040210	0.047740895083618	0.03418135091785
23	0.00001434360003	0.00051636960118	0.023118940975986	0.01605482012221
Thigh	Average BCS	Average MCS	Total mass	Total Inertia
Shank	0.00124174594569	0.01008157402067	3.59114430270976	0.07717524619818
Foot	0.00058367418595	0.00353566356646	2.46243823710496	0.53961319293813
Total BCS	Total MCS	Total mass	Total Inertia	
Complete Leg	0.01726969443952	0.12316138772389	6.40191870553499	0.83210567381874
Leg(+5% foot)	0.01728332085955	0.12326824754413	6.40738825293724	0.83592670458416
Leg(-5% foot)	0.01725606801949	0.12305452790364	6.39645115813273	0.83592670458416

As we can see the +5% foot mass has an insignificant effect on the total mass and total inertia. An explanation of this is that the leg is not well adapted to cursory, so what might have a larger significance on a agile fast animal does not have the same impact on *Falcarius*. In addition Pontzer outlined two methods for estimating the cost of transport (COT) in extant animals, one based off of total mass, and the second based off of effective limb length (the length of the limb in the y direction when the animal is standing) (Pontzer, 2007). The regression is derived over a wide variety of extant animals to average the results. However since one is based off of the geometry of the animal, and the other is simply based off of mass, then the relationship between these two results can give us insight to cursorial adaptations of *Falcarius*. When we use the mass COT  $y=11.259x^{-0.26}$  (Pontzer, 2007) with *Falcarius*' mass of 100 kg (Paul, 2010) we get that COT= 3.40, and if we use the effective limb length,  $y=90.284x^{-0.77}$  we get that COT= 3.42. Now since when we take into account the geometry of *Falcarius* the COT is higher than if we just consider mass, we can infer that *Falcarius* did not have cursorial adaptations, in fact, it probably had about average movement capabilities. This means that it probably had cursorial regression from the formerly well adapted theropod group which it evolved from.

Figures:



Copyright Scott Hartman, 2011.

Fig HR.1, a reconstruction of *Falcarius* by Hartman done for the UMNH, available on his blog at <http://skeletaldrawing.blogspot.com/2011/11/falcarius-bizarre-sickle-cutter.html>

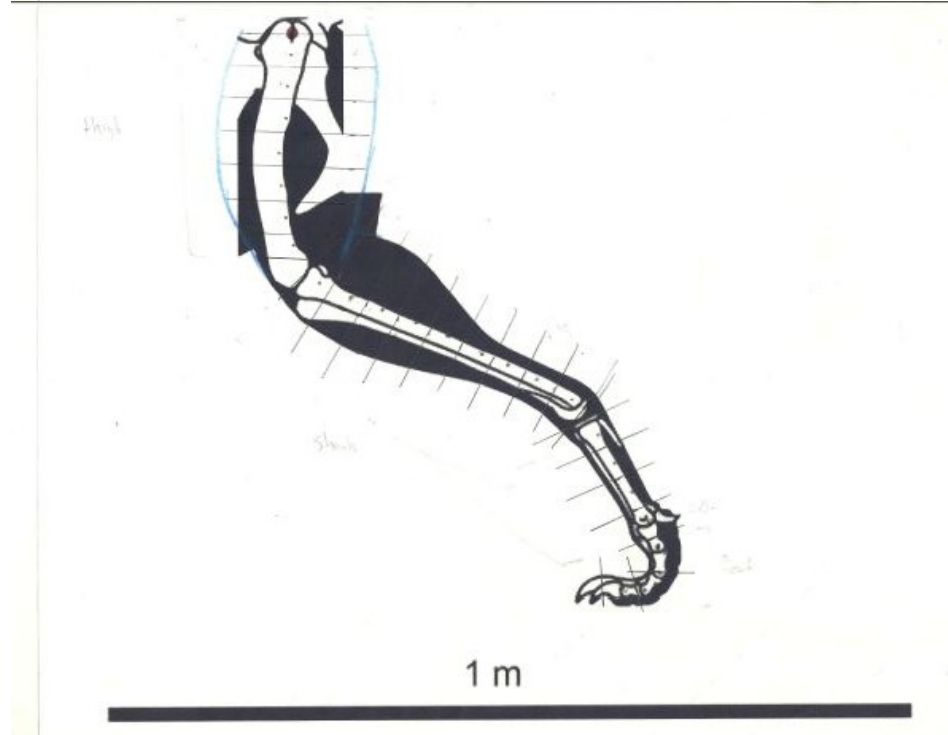


Fig HR.2, the sectioned limb. The center of mass was assumed to be at the dot.

### Assumptions

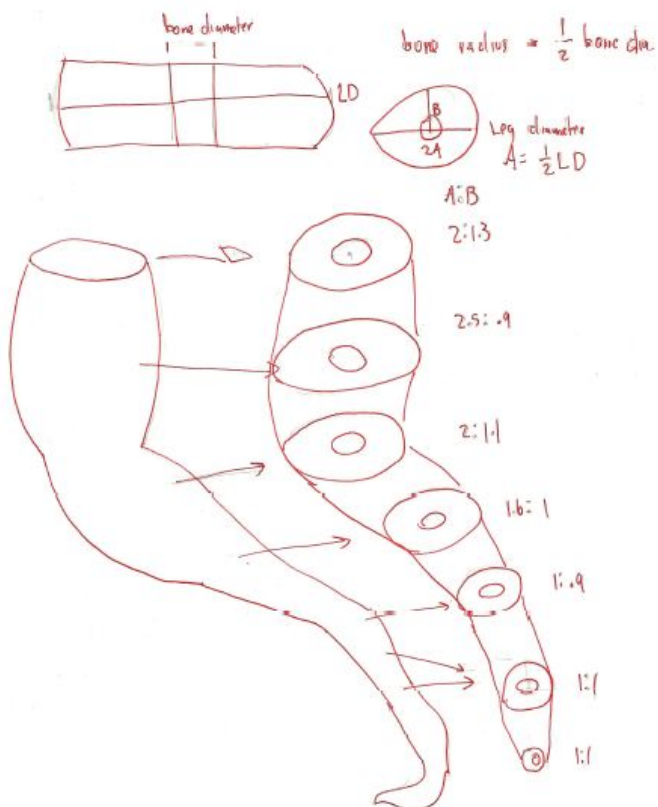


Fig HR.3, the proportions assumed for the hindlimb.

### Muscle Reconstruction

#### Methods and Material:

To reconstruct the muscle *M. caudofemoralis* in *Falcarius* we note that since *Falcarius* was a non-avian dinosaur it is likely that the muscle *M. caudofemoralis* originated from a transverse process as well as the vertebral central, and inserted on the fourth trochanter of the femur and probably inserted on the proximal tibia. This is based off of the anatomy of extant crocodilians. (Schachner, 2011).

Based off of muscle scarring on the transverse process, we can tell that *M. caudofemoralis* originated from the 10th vertebra behind the pelvis (Zanno , 2010) (see figure MR.1).

#### Results:

As we can see, *M. caudofemoralis* took up less than a third of the total length of his tail (see figure MR.2) . Typically in extant reptiles the muscle extends to about half of the tail length (Persons, 2011). Considering the fact that the primary role of this muscle is as hindlimb retractor, it is likely that *Falcarius* did not have the muscle mass needed for high move speeds (Persons, 2011).

Figures:

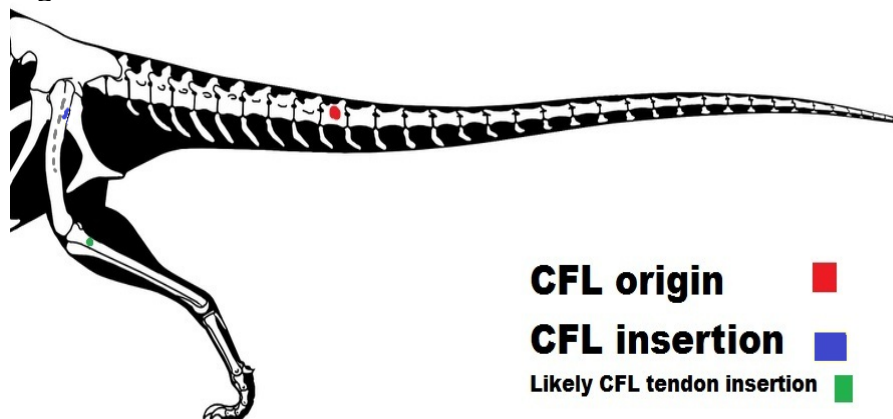


Fig MR.1. Note since the reconstruction is done from a lateral perspective, and it inserts onto the medial surface, I have added a dashed line to indicate a shift from the latter surface to the former just on the muscle map, not the reconstruction.

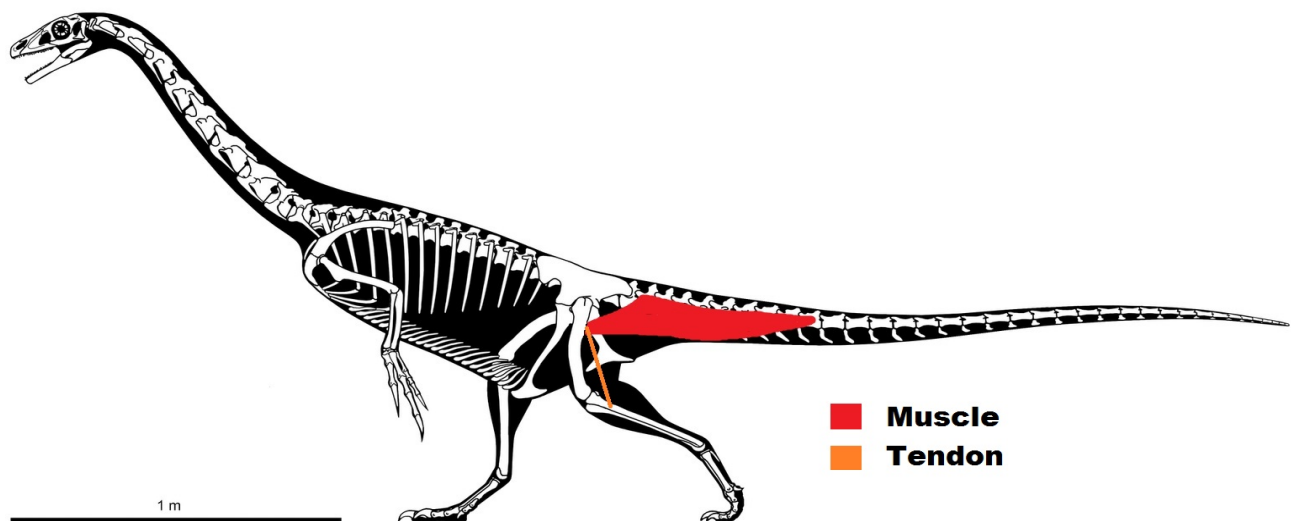


Fig MR.2 The full muscle reconstruction.

## Auditory Reconstruction

### Methods and Materials:

An inner ear reconstruction was available via CT scan and using Surf Driver 8 (Smith, 2011). For exact methodology see (Smith, 2011). This reconstruction allowed us to compare the cochlear duct (see fig AR.1) in *Falcarius* to that of extant birds and reptiles to predict the mean auditory frequency range (Walsh, 2008). While Walsh outlines a method for determining auditory range based off of endosseous cochlear duct (ECD) length, he uses a normalization factor that is unclear and ill defined in that paper. However he published his original, unnormalized data. So we used a small sample of his data to create a simple linear regression, based off of ECD length and

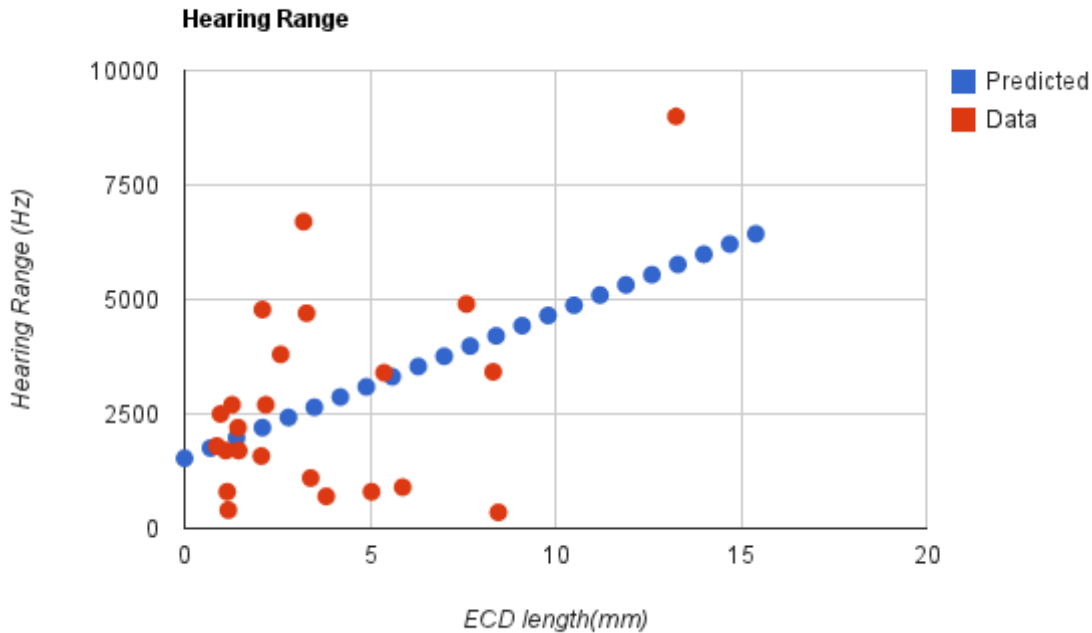
hearing range in extant reptiles and birds. For the exact materials and methods used to gather the hearing sensitivity data see (Walsh, 2008).

### Results:

The data from Walsh that we used was the following:

Species	Length(mm)	Overall range (Hz)
<i>acutus</i>	1.28	2700
<i>mississippiensis</i>	5.88	900
<i>crocodylus</i>	<b>1.11</b>	1700
<i>mydas</i>	8.46	350
<i>serpenta</i>	5.04	800
<i>punctatus</i>	3.82	700
<i>gecko</i>	2.1	4780
<i>hasselquistii</i>	<b>1.44</b>	2200
<i>caudicinctus</i>	2.07	1580
<i>scicula</i>	0.97	2500
<i>rugosa</i>	2.59	3800
<i>occelatus</i>	<b>1.46</b>	1700
<i>niloticus</i>	3.4	1100
<i>wislizenii</i>	<b>1.18</b>	400
<i>sagrei</i>	0.87	1800
<i>hardwickii</i>	<b>2.19</b>	2700
<i>zarudnyi</i>	1.15	800
<i>alba</i>	<b>13.25</b>	9000
<i>undulatus</i>	<b>3.21</b>	6700
<i>novaehollandiae</i>	8.32	3420
<i>demersus</i>	5.38	3400
sp.	7.6	4900
<i>guttata</i>	3.29	4700

Our regression looks like the following:



When we use the ECD length of 10.1 for *Falcarius* (Fig AR.1) (Smith, 2011) we get a predicted hearing range around 4750 Hz. This ECD length is a lot higher than in other similar theropods, such as *Allosaurus* and *Ceratosaurus* (Smith, 2011). This suggests that *Falcarius* could have heard a large range of frequency which may have included sounds made by juveniles, prey, other small bodies, and adults (Smith, 2011). In addition, there is a positive correlation between hearing range frequency and sociability, so there is a chance that *Falcarius* lived in larger aggregates (Walsh, 2008). While this data could imply either predatory behavior, since a larger frequency range could aid hunting behaviors, or herbivorous behavior, since it would enable hearing as a defence mechanism, it implies more of a specific mechanism on how either would work. Moreover, it could likely imply either a pack or herd structure.

Figures:

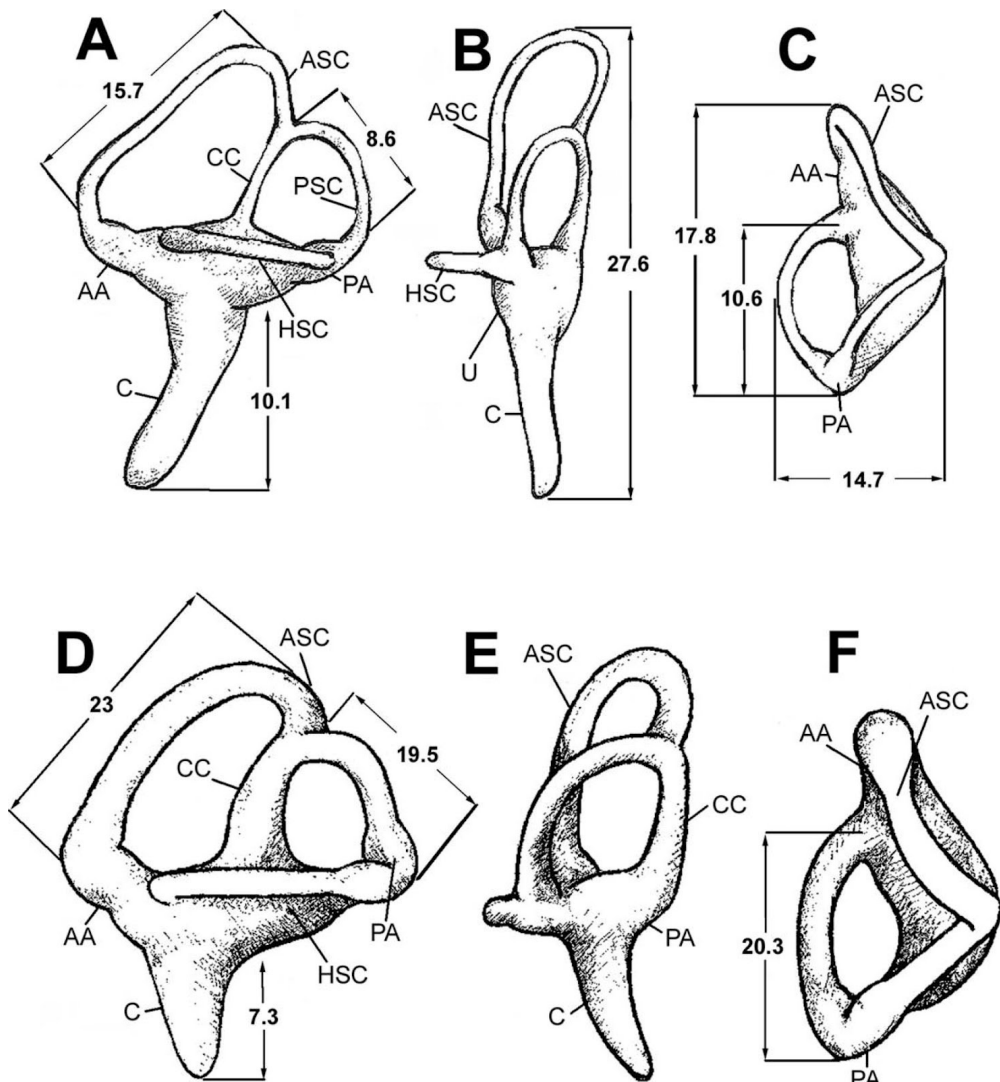


Fig AR.1. *Falcarius* courtesy of (Smith, 2011)

**Anatomical Abbreviations**—AA, anterior ampulla; ASC, anterior semicircular canal; C, cochlear duct; CC, common crus; HSC, horizontal semicircular canal; PA, posterior ampulla; PSC, posterior semicircular canal; U, utricle;

### Cardiovascular and Respiratory reconstruction

#### Materials and Methods:

(Blaylock, 2000) outlines many allometric curves for various cardiovascular and respiratory quantities. These include the stroke volume of the heart (SV), amount of oxygen used (VO<sub>2</sub>), heart rate (HR), and heart mass (using the method of Laplace for stress) (Blaylock, 2000). For the exact methods used see (Blaylock, 2000). We used these quantities, along with some endothermic and endothermic assumptions to model the mean arterial pressure (MAP), the oxygen extraction rate, and the heart mass (assuming a spherical heart with thin walls). In addition, we ran a sensitivity analysis by changing the mass +15%.

Our assumptions were that endotherms have an intracranial pressure of 90 mmHg and ectotherms have an intracranial pressure of 40 mmHg. With this information, the distance between the center of the heart and the center of the head (determined to be 1.17m for *Falcarius*), and the density of blood (assumed to be 1055 kg/m<sup>3</sup>), we can determine MAP. To determine this, we used conservation of energy applied to pressure, and the assumption that MAP is uniform throughout the body. Then we get that  $MAP = ICP + p \cdot h \cdot g$ , where ICP is the inter-cranial pressure, p is the density of blood, h is the distance from the heart to the head, and g is the acceleration due to gravity.

To determine oxygen extraction ( $Ca - Cv$ , where  $Ca$  is the concentration of oxygen in arterial blood, and  $Cv$  for venous blood) we used Fick's principle, which is  $(Ca - Cv) * SV * HR = VO_2$ , and the allometric data for HR, SV and  $VO_2$  (Blaylock,2000).

Finally, to estimate heart volume we assumed that the heart was a sphere with the inner radius, r, and thickness, t. Then we assumed that the maximum volume was  $1.5 * SV$ . Using this we can determine radius. Then using a thin wall assumption (stress = pressure \* radius / (2 \* thickness)), and assuming exterior stress is 20kPa, we can determine thickness. Then with heart volume we can determine the mass, assuming the density of muscle = 1006 kg/m<sup>3</sup>.

### Results:

We got the following results for  $VO_2$  (mL/min)

Mass(kg)	Bird	Mammal	Reptile
85	276.86	339.48	38.4
100	311.23	384.11	43.3
115	344.17	427.16	48.0

For endotherms we got that  $MAP = 180.74$  mmHg, and for ectotherms  $MAP = 130.74$

For oxygen extraction (unitless) we got the following ranges over 85-100 kg

Bird	Mammal	Reptile
.04	.0487-.0488	.06496-.0654

Then interesting results was that when we substituted the allometric curves into Fick's equation we get that the oxygen extraction for birds does not scale with mass, for mammals its proportional for  $m^{-0.01}$  and for reptiles  $m^{-0.02}$ . This could be a result of range of masses of the tested animals, or different physiologies (difference in avians lungs against mammalian lungs).

For Heart Rate (beats/minute)

Mass(kg)	Birds	Mammal	Reptile
85	57.6	81.7	6.9
100	55.1	77.7	6.64
115	53.0	76.2	6.41

Stroke Volume (mL)

Mass (kg)	Birds	Mammal	Reptile
85	119	85	85

100	140	100	100
115	160	115	115

Heart mass/ Total Mass (as a %) using thin wall assumption

Mass (kg)	Bird(endo)	Bird(ecto)	Mammal(Endo)	Mammal(ecto)	Reptile(endo)	Reptile(ecto)
85	0.66	0.41	0.47	0.29	0.47	0.29
100	0.66	0.42	0.47	0.30	0.47	0.30
115	0.64	0.42	0.47	0.30	0.47	0.30

Heart mass/ Total mass (as a %) with the method of Laplace (Blaylock,2000).

Mass(kg)	Bird	Mammal	Reptile
85	0.542	0.527	-
100	0.534	0.53	-

115	0.527	0.537	-
-----	-------	-------	---

Oxygen levels present in the atmosphere 125 million years ago would have been about 2-3% higher than today's level (Berner, 1999). This means that there is a high likelihood that the lungs needed at that period would have been comparable to that in extant animals, in terms of membrane thickness and volume, possibly marginally less since oxygen extraction would have been easier. Since these level are fairly similar, the data generated by the allometric curves in extant animals should be viable for *Falcarius*.

The data generated seems to support two possible variations of cardiovascular and respiratory physiologies. The first kind would support high amount of activity (modeling *Falcarius* with either mammalian or avian mechanics). Either assumption would make the heart mass approximately equal (using the method of Laplace). To provide adequate oxygen supply using mammalian mechanics the internal lung surface area would have had to be ~25% larger, or had ~25% thinner membranes, or some combination of the two. In addition to support a higher VO<sub>2</sub> max, the heart rate would need to be ~33% larger in mammalian mechanics than in avian mechanics. The avian hearts would take up a significantly more volume than mammalian heart, but it would have a larger stroke volume.

It's likely that both hearts would have had contained a divided ventricle, since it is present in both extant birds and mammals, both of which have the highest VO<sub>2</sub> outputs of extant animals.

The second variation would support low levels of activity (modeling *Falcarius* with reptilian mechanism). The lungs would have need to be able to supply ~50% more than the avian lung, which would probably require both thinner membranes and an increase in internal surface area. The high levels of oxygen would have helped facilitate this, and dampened the needed volume. However the heart would have needed to be significantly smaller to supply the required amount of oxygen and pressure. This means that there is a good chance that the heart would have only needed one ventricle.

However there is little evidence that *Falcarius*, and theropods in general, would have had avian lungs (Quick, 2007). In addition, it was likely that theropods had a cardiovascular system similar to crocodilians (Quick, 2007). This means that *Falcarius* would have had a four-chambered heart or a five-chambered heart, which would have allowed oxygenated blood and deoxygenated blood to mix (Quick, 2007). This implies that *Falcarius* would have had the latter discussed variation, that supported low level of activity, as seen in extant reptiles.

## Bite force Estimation

### Materials and methods:

A A Z&F 5600i laser scanner was used to digitize a juvenile skull of *Alligator mississippiensis*. To investigate bite force we used the MDA package GaitSym. Upper and lower jaw segments were connected with one hinge. We reconstructed the basic muscle system, with the physical cross sectional area outlined in (Porro, 2011). Finally

we tested the bite force generated at the end of the snout in our model, as well as where the teeth start to generate a range of maximal bite force.

### Results:

Our results were that the bite force of a juvenile *Alligator mississippiensis* could range from 150- 250N , based on the position where bite force is measured. This is consistent with results done in similar experiments, see (Bates,2012). *Falcarius*' snout length was approximately ~0.25 m , while the snout length of our skull model was ~0.2 m. Since they are approximately the length, we can assume that the muscle cross sectional area is roughly the same, and that *Falcarius* would have a bite force that is a 25% increase of that of a juvenile alligator. This would put the range of *Falcarius*' bite force to be 190-310 N. For comparison, the human bite force range is 700-1020N (Bates, 2012) .

While this does not rule out *Falcarius* as primarily a predator, it does eliminate a biting mechanism as a potential predatory mechanism.

### Conclusion

Many of the traits that were analyzed in *Falcarius* allude to it being herbivorous. While no single trait that was analyzed excludes predatory behavior, none of them suggest it. The hindlimb reconstruction along with the M. caudofemoralis reconstruction both support the hypothesis that this dinosaur was not capable of high running speeds. This fact in symphony with the cardiovascular and respiratory reconstruction, suggests a slow moving, lethargic dinosaur. Furthermore, the low bite force suggests no predatory behavior short of scavenging, since there would be no viable way for *Falcarius* to hunt or injure prey. Finally it was highly unlikely that it scavenged, due to the extremely well adapted inner ear structure. While a large hearing range could facilitate in the survival of a slow scavenger, based off of the other traits it was likely that the structure supported a social structure. Ultimately, it seems likely that *Falcarius* was primarily herbivorous and lived in a large social aggregate.

### References

Bates, Karl T., Falkingham, Peter L., Breithaupt, Brent H., Hodgetts, David, Sellers, William I., and Manning, Phillip L., 2009. How Big Was 'Big Al'? Quantifying the effect of soft tissue and osteological unknowns on mass predictions for Allosaurus (Dinosauria:Theropoda). *Palaeontologia Electronica* Vol. 12, Issue 3; 14A: 33p;  
[http://palaeo-electronica.org/2009\\_3/186/index.html](http://palaeo-electronica.org/2009_3/186/index.html)

K. T. Bates and P. L. Falkingham. Estimating maximum bite performance in *Tyrannosaurus rex* using multi-body dynamics Biol Lett 2012 : rsbl.2012.0056v1-rsbl20120056.

Robert A. Berner .Atmospheric oxygen over Phanerozoic time. PNAS 1999 96: 10955-10957.

Brøndum, E. Jugular venous pooling during lowering of the head affects blood pressure of the anesthetized giraffe. American journal of physiology. Regulatory, integrative and comparative physiology 297.4 (2009):R1058.

Hutchinson JR, Bates KT, Molnar J, Allen V, Makovicky PJ (2011) A Computational Analysis of Limb and Body Dimensions in *Tyrannosaurus rex* with Implications for Locomotion, Ontogeny, and Growth. PLoS ONE 6(10): e26037. doi:10.1371/journal.pone.0026037

Falkingham, Peter L. 2012. Acquisition of high resolution 3D models using free, open-source, photogrammetric software. *Palaeontologia Electronica* Vol. 15, Issue 1; 1T:15p;

Kirkland, James I. A primitive therizinosauroid dinosaur from the Early Cretaceous of Utah. *Nature* 435.7038 (2005):84.

Paul, G.S., 2010, *The Princeton Field Guide to Dinosaurs*, Princeton University Press p. 156

Persons, W S. "The tail of *Tyrannosaurus*: reassessing the size and locomotive importance of the *M. caudofemoralis* in non-avian theropods." *The anatomical record* 294.1 (2011):119.

Schachner, Emma R. "Pelvic and hindlimb myology of the basal Archosaur *Poposaurus gracilis* (Archosauria: Poposauroidea)." *Journal of morphology* 272.12 (2011):1464.

Seymour R, Blaylock A. The principle of Laplace and Scaling of Ventricular Wall Stress and Blood Pressure in Mammals and Birds. *Physiological and Biochemical Zoology*, Vol. 73, No. 4 (July/August 2000), pp. 389-405

Smith, David K. "New Information on the Braincase of the North American Therizinosaurian (Theropoda, Maniraptora) *Falcarius utahensis*." *Journal of Vertebrate Paleontology* 31.2 (2011):387-404.

Porro, L. B., Holliday, C. M., Anapol, F., Ontiveros, L. C., Ontiveros, L. T. & Ross, C. F. 2011 Free body analysis, beam mechanics and finite element modelling of the mandible of *Alligator mississippiensis*. *J. Morph.* 272, 910–937. (doi:10.1002/jmor.10957)

Quick, Devon E. "Cardioa pulmonary anatomy in theropod dinosaurs: Implications from extant archosaurs." *Journal of morphology* 270.10 (2009):1232-1246.

Walsh, S., P. Barrett, A. Milner, G. Manley, and L. Witmer. 2008. Inner ear anatomy is a proxy for deducing inner ear capability and behaviour in reptiles and birds. *Proceedings of the Royal Society B* 1390:1–6.

Zanno.L.E 2010 .Osteology of *Falcarius utahensis* (Dinosauria: Theropoda): characterizing the anatomy of basal therizinosaurs. *Zool. J. Linn. Soc.* :196-230.

Zanno, L. E. The pectoral girdle and forelimb of the primitive therizinosauroid *Falcarius utahensis* (Theropoda, Maniraptora): analyzing evolutionary trends within Therizinosauroidae. 2006. *Journal of Vertebrate Paleontology* 26:636-650.

Zanno, Lindsay E. A new North American therizinosaurid and the role of herbivory in 'predatory' dinosaur evolution. *Proceedings - Royal Society. Biological sciences* 276.1672 (2009):3505.

## Installation appendix

Instructions(to get python, but **just** python, dont download the osm bundler):

<http://code.google.com/p/osm-bundler/wiki/InstallingRunningApplication>

Downloads(the one we want is osm-bundler-pmv2-full-32-64, and the example photos if you want to test it out on those):

<http://code.google.com/p/osm-bundler/downloads/list>

Getting python to work in the command prompt <http://showmedo.com/videotutorials/video?name=960000&fromSeriesID=96>

Got meshlab

<http://sourceforge.net/projects/meshlab/files/>

### Things we need first

- python ( you need version 2.7)
- the PIL library
- the osm-bundler-pmv2-full-32-64
- photos to test

First things first

- downloading and install python, then the PIL library, this should be straightforward( provided by the link above)
- unzip the download and put them in a convenient spot, you want the photos in the osm-bundler file under the osm-bundlerWinXX subfolder (for me XX=64, because im on a 64 bit machine, if you dont know this, its probably 32 if its older, 64 if its newer and nice, 32 if its newer and not so good)
- now that folder should have osmbundler, osmcmvs, osmpmvs, software, testPhotos (this is what i called the folder of my photos), and three python scripts RunBundler.py, RunCmvs.py, RunPMVS.py
- goto start menu and type in cmd

- find the directory you unzipped the osm-bundler software

for me its "C:\Users\Geoff\Desktop\photogrammetry\osm-bundler-pmv2-cmvs-full-32-64\osm-bundlerWin64"

We need to tell the computer where our python scripts and photos are located at  
so enter the command

```
cd C:\Users\Geoff\Desktop\photogrammetry\osm-bundler-pmv2-cmvs-full-32-64\osm-bundlerWin64
```

Now we need to tell computer to run our python scripts

First try typing in python and hitting enter, if it doesnt pop up with the version then you need to follow the link above to get python to work in the cmd

If it changes the line entry from C:\ourDirectory to >>> then just hit control+z, then hit enter and it should return you

now that python works, we need to tell the computer to run out python script in python so enter the command

**python RunBundler.py --photos=testPhotos** (or whatever folder you called it)

Let that run, then a folder should pop up, and we need to get the file directory of that folder now we need to run the second python script

For this example we are going to use the PMVS script, for many photos you change it to the CMVS, but I currently haven't tested how this works

Now we need to run the second script on the output that it just created so we do the following

**python RunPMVS.py --bundlerOutputPath=C:\User\Geoff\AppData\Local\Temp\osm-bundler-wdjsxc**

Now in MeshLab, go to importMesh, go to that long folder in the temp data, go to pmvs, models, and the file that is in there, and voila!

Note: If it doesn't support your camera type, then you will have to edit it with this

<http://sourceforge.net/projects/sqlitebrowser/>

Then open that, and open the file osm-bundler-pmv2-cmvs-32-64/osm-BundlerWin64/osmbundler/cameras

Then change one of the cameras to reflect your camera, here is a list of stats that i found

[https://svn.personalrobotics.ri.cmu.edu/public/trunk/src/moped/BundlerPy/bin/extract\\_focal.pl](https://svn.personalrobotics.ri.cmu.edu/public/trunk/src/moped/BundlerPy/bin/extract_focal.pl)